35th Annual International Conference of the IEEE EMBS
Osaka, Japan, 3 - 7 July, 2013

Imaging and Estimation of Human Abdominal Fat by Electrical Impedance Tomography Using Multiple Voltage Measurement Patterns

Tohru F. Yamaguchi[1], Mitsuhiro Katashima[1],
Li-qun Wang[2] and Shinya Kuriki[2]

Abstract— **A measuring device for human abdominal fat from the conductivity image derived by electrical impedance tomography (EIT) is rarely found. This study was aimed to reconstruct precise conductivity images from multiple voltage measurements in different patterns of the combination of current and voltage electrodes. We examined two voltage measuring patterns using electrodes located at upper and lower levels around the abdomen of a subject. In the experiment, after 1024 voltage data were taken from one specified voltage measurement pattern, another 1024 data were also taken continuously using another pattern. The reconstruction of conductivity image was made using entire data. As a result, the tomography image was improved compared with the image obtained from single voltage measurement pattern. We then obtained the histogram of the conductivities and estimated the area of abdominal fat. The present method using multiple voltage measurement patterns would be effective, if the measuring time can be much reduced through future modification of the tomography device.**

I. INTRODUCTION

The epidemic of metabolic syndrome is a serious health problem worldwide [1]. The fundamental cause of metabolic syndrome is thought to be an accumulation of abdominal fat [2], especially visceral fat [3]. Although the standard method for estimating abdominal fat is to analyze the tomography image acquired from X-ray CT or MRI [4], these devices have disadvantages such as introduction and maintenannce costs. Furthermore, in the case of X-ray CT, inevitable radiation exposure is a serious problem [5], [6] during health check-ups.

Electrical impedance tomography (EIT) is a non-invasive and relatively low-cost imaging method [7], [8]. This method involves several technical problems in its instrumentation and image reconstruction. Therefore, its utilization in the medical field is very limited. We have succeeded to obtain the image of absolute conductivity of human abdomen [9]. However, the current technique was not acceptable for quantitative imaging of visceral fat, which is more relevant to human health [10]. The main reason for this is thought to be the limited number of independent data of measured impedance.

In this study, we attempted to obtain more precise image of the conductivity from many data using multiple voltage measurement patterns of voltage measurement. Then, we attempted to do quantitative estimation of abdominal fat using our proposed method.

[1]T. Yamaguchi and M. Katashima are with Health Care Food Research Laboratories, Kao Corporation, 131-8501 Tokyo, Japan yamaguchi.tohru@kao.co.jp, mitsuhiro.katashima@kao.co.jp

[2]L. Wang and S. Kuriki are with The Research Institute for Science and Technology, Tokyo Denki University, Chiba, 270-1382, Japan wang@rcat.dendai.ac.jp, skuriki@rcat.dendai.ac.jp

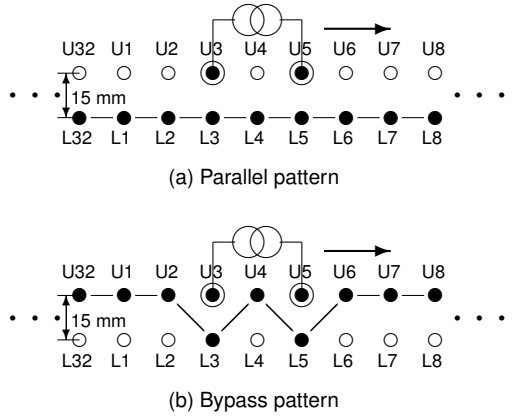

Fig. 1. Data acquisition using two voltage measurement patterns. Electrodes indicated by solid circle, in the upper and lower levels were used to measure voltages while the current source was connected to U3 and U5 electrodes located in the upper level.

II. METHOD

A. Apparatus

The measuring device was designed to obtain human abdominal fat image. We prepared two circular electrode arrays separated vertically in 15 mm. Those electrodes were equidistantly arranged at 32 locations along the ring and gently pushed by low friction air cylinders to a subject's abdomen. Simultaneously, the movements of cylinder rods were measured by position sensors; therefore, the subject's abdominal outline shape and cross-sectional area could be measured. The electrodes located in the upper level served as the current injection electrodes or voltage measuring electrodes by flicking the electro-magnetic relay switch, and the lower level electrodes served as voltage measuring electrodes only (Fig. 1).

Probing signal source can be connected to any electrodes in the upper level through push-pull type constant current circuits located at each electrode station. Voltage measurement was designed to measure the potential difference between every adjacent electrodes using an instrumentation amplifier. The signal was transferred to a phase-sensitive demodulator

978-1-4577-0216-7/13/$26.00 ©2013 IEEE

(CD-552R4, NF Corporation, Yokohama, Japan) composing lock-in amplifier to measure the real part of complex impedance; and that was converted to direct current (DC) signal. Finally, this DC signal was measured with a digital multi meter that had 6.5 digits in the dynamic range. The mechanics and electronics were controlled by a PC, where the control program was programmed by C language (LabWindows/CVI, National Instruments, Austin, TX).

B. Data acquisition

The interval of the current electrodes was fixed as two units in this study. After the measurement of voltages, the pair of current electrodes was shifted to the next pair until the pair went to one round in 'parallel' pattern, as shown in Fig. 1. Then, another one round measurement was made for the different measurement pattern in 'bypass' pattern. In both patterns, seamless potential difference in a closed-loop was measured. Therefore, the summation of those 32 voltages in one round should be zero taking into account their signs. We utilized this relationship to correct the recorded voltage data, namely we subtracted the summation of the data divided by 32 from each datum.

C. Image reconstruction

The image was reconstructed by iterative calculation for a forward problem and an inverse problem. We used a three-dimensional finite element method (FEM) to solve the forward problem. The computer model used in this calculation had 708 elements in the cross-section and 12 layers in the longitudinal direction. Each element had electrical conductivity of the transverse direction and longitudinal direction considering bio-electrical anisotropy. The mesh was fixed mesh, and the distance from the center to the boundary was stretched depending on the subject's outline shape, which was directly measured, and the longitudinal direction was 500 mm long. The model was assumed to be homogeneous in the longitudinal direction geometrically and electrically. Therefore, the number of unknown parameters was two anisotropic conductivities of 708 elements. However, we assuming certain dependency in the boundary elements, the number of unknown parameters to be estimated was reduced to two of 420 (= 840). In the forward calculation, we calculated not only potentials at nodes but also the sensitivity of elements defined by the differential of the change in voltage and a change in conductivity using Geselowitz's theorem [11]. This sensitivity was used to solve the inverse problem of the backward conductivity updating. We defined the sensitivity matrix with its element of the sensitivity, where the row size was the number of data and column size was the number of unknown conductivities. Then the sensitivity matrix was decomposed by the singular value decomposition to obtain a transformation matrix. The conductivity updating was calculated in a shrunk space converted by the conversion matrix to exclude the negative effect of the small absolute value of singular value. Refer to Yamaguchi et al. [9], [12] for further details of the computation.

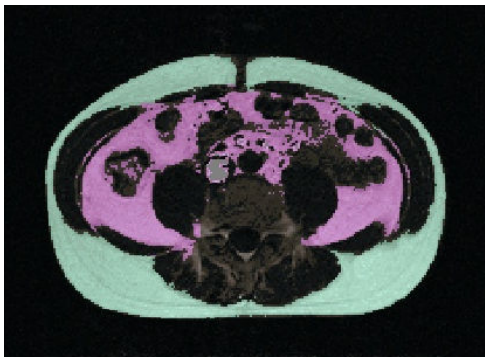

Fig. 2. Abdominal MR image of subject (one of the authors of this study). The abdominal subcutaneous fat and visceral fat are indicated as green and pink colors, respectively.

The image reconstruction method was programed using **R** language [13]. Some subroutines used parallel computation or were programmed using FORTRAN77 in consideration of computation speed.

D. Estimation of abdominal fat area

In the case of X-ray CT and MRI, fat area estimation is performed by segmentation of image basically by their brightness of pixels (Fig. 2). In the case of EIT, it is not possible to segment each pixel, because of the low resolution. Therefore, we developed an original method to estimate the fat area.

In a histogram of conductivity of pixels after spatial filtering from the calculated conductivity image, two peaks were found in around 0.02 S/m and 0.1 S/m. We thought that the former peak corresponded to the body fat component, and latter peak non-fat component. Then we applied a truncated two-component mixed distribution model for the distribution of conductivity as in Eq. (1).

$$f(z|\theta) = \frac{1-\lambda}{G_1(b)-G_1(a)} g_1(z) + \frac{\lambda}{G_2(b)-G_2(a)} g_2(z) \quad (a \le z \le b) \tag{1}$$

where g_1 and g_2 are probability density functions (PDFs), and G_1 and G_2 are cumulative distribution functions for the two components. We used logarithmic skew-normal distribution [14] for the two PDFs of the two components. Then we estimated the model parameters (θ) including the mixed ratio (λ) of body fat using the maximum likelihood method. Finally, total body fat area was calculated from the product of cross-sectional area and λ.

E. Experimental procedure

This experiment was conducted after the approval of the ethical committee of Tokyo Denki University (Tokyo, Japan) and was conformed to the spirit of the Declaration of Helsinki. The subject was one of the authors.

Before the measurement, an ordinary moisture cream was applied to the tip of dry stainless-steel electrodes. The

probing current of 1.0 mA_{rms} and 500 kHz in frequency was applied to the subject's umbilical level. The current electrode interval was two units, and the voltage measurement pattern was parallel and bypass. The measurements in the two patterns were carried out continuously, lasting for about 40 minutes. The subject maintained a stable posture with normal breathing during the measuring period. Then the image reconstruction and fat area estimation were made. This took about two hours using a conventional PC equipped Intel® Core 2 Duo® processor, the base clock frequency of which was 2.4 GHz.

III. RESULTS

A. Reconstructed image

Fig. 3 shows a plot of singular values decomposed from the sensitivity matrices. Comparing the two patterns' datasets and the combined dataset, the combined dataset had slightly more large singular values.

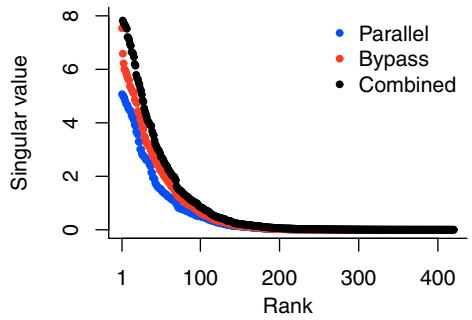

(a) Transverse direction

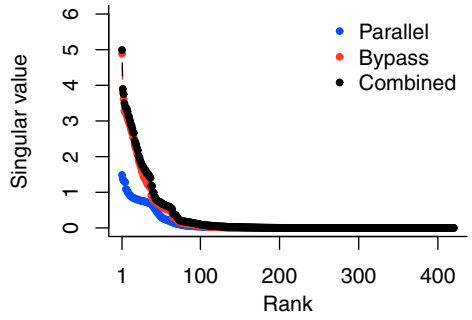

(b) Longitudinal direction

Fig. 3. Comparison of the singular values decomposed from the sensitivity matrix of 'parallel' pattern dataset, 'bypass' pattern dataset, and 'parallel' and 'bypass' patterns combined dataset for uniform conductivities. The Y-axis shows absolute values of the singular value sorted in descending order, and X-axis shows their ranks.

Fig. 4 shows reconstructed images of average conductivity derived from anisotropic conductivities of transverse and longitudinal directions. Panels (a) and (b) show reconstructed images from the parallel pattern dataset and bypass pattern dataset, respectively, and panel (c) shows an image from both patterns datasets. The obtained conductivity from 0.01 S/m to 1.0 S/m is within the range of physiologically plausible values [15], [16], which is indicated in the scale of image.

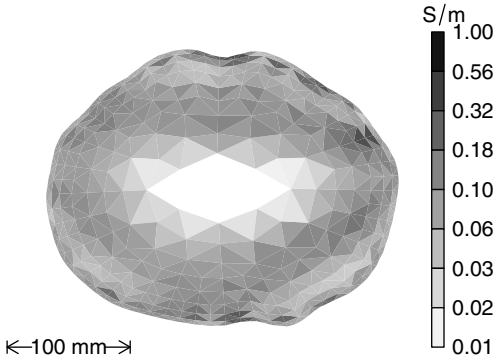

(a) Image reconstructed from 'parallel' pattern dataset.

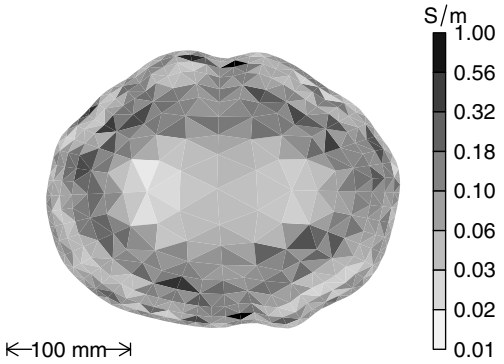

(b) Image reconstructed from 'bypass' pattern dataset.

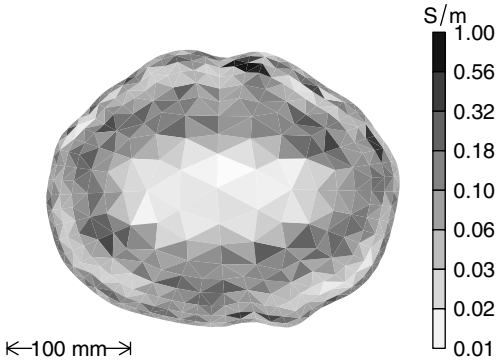

(c) Image reconstructed from both 'parallel' and 'bypass' patterns combined dataset.

Fig. 4. Abdominal EIT images.

Comparing with the abdominal MR image (Fig. 2) of the same subject, it may be possible to identify the abdominal subcutaneous fat, abdominal muscles and abdominal cavity in the EIT image (Fig. 4c).

B. Estimated fat area

Fig. 5(b) show the histogram of the conductivities derived from the spatially filtered image (Fig. 5a). The estimated λ was 0.25. The abdominal fat area was estimated to be 127 cm^2, while an area of 202 cm^2 was estimated from the image analysis of MRI.

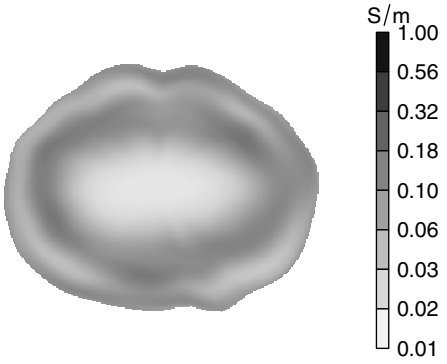

(a) Spatially filtered image.

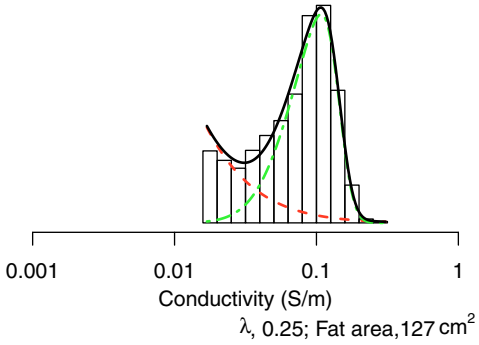

(b) Histogram of spatially filtered conductivity data.

Fig. 5. Estimation of abdominal fat area using truncated two component mixed distribution model. Dashed and dotted lines show fitted probability density functions of two components, and solid line shows the mixed distribution.

IV. DISCUSSION

The conductivity in Fig. 4(c) was in the physiologically plausible range (Fig. 5b) whereas the conductivity in the central abdominal region was out of the range without the anisotropic model [12]. The abdominal subcutaneous fat, abdominal muscle, and abdominal cavity were identified, although the structure in the abdominal cavity was not clear.

The reciprocal theorem and/or the principle of superposition hold in the data collected from the ring-arrangement of electrodes. In this study, we used two voltage measurement patterns i.e., parallel and bypass patterns, which means that all of 64 electrodes were employed to inject the current or to measure the voltages. In the bypass pattern, the level of voltage measurement electrodes was almost the same as the level of current injection electrodes, while it was different in the parallel pattern. Thus, we could obtain more information about subject's abdominal conductivity in simultaneous measurements of parallel and bypass patterns. Accordingly, the results shown in Fig. 3 and Fig. 4(c) suggest the better image could be derived by the image reconstruction from both patterns dataset. However, the estimated fat area obtained in our proposed method is much smaller than that of MRI. The estimated fat areas with another three subjects in the previous study [12] reflected different degrees of abdominal fat accumulation but also showed underestimation. It may be due to uncertain estimation of conductivities in the abdominal cavity.

The main disadvantage of using multiple measurement patterns is long measuring time. In our device setup, it took more than 40 minutes to collect a dataset of two patterns. That may not practical to be included as a part of check-up in a hospital. Therefore, the design of instrumentation needs modification. A parallel voltage measurement using many lock-in amplifiers and high-resolution A/D converters may be helpful.

V. CONCLUSIONS

It was suggested that the method using multiple voltage measurement patterns would be effective to improve estimation of abdominal conductivity and abdominal fat area. This method is radiation-free and may be practical if the measuring time can be much reduced through future modification of the tomography device.

REFERENCES

[1] M. A. Cornier, D. Dabelea, T. L. Hernandez, R. C. Lindstrom, A. J. Steig, N. R. Stob, R. E. Van Pelt, H. Wang, and R. H. Eckel, "The Metabolic Syndrome," *Endocr Rev*, vol. 29, no. 7, pp. 777–822, 2008.

[2] J. P. Després and I. Lemieux, "Abdominal obesity and metabolic syndrome," *Nature*, vol. 444, no. 7121, pp. 881–887, 2006.

[3] Y. Okauchi, H. Nishizawa, T. Funahashi, T. Ogawa, M. Noguchi, M. Ryo, S. Kihara, H. Iwahashi, K. Yamagata, T. Nakamura, I. Shimomura, and Y. Matsuzawa, "Reduction of visceral fat is associated with decrease in the number of metabolic risk factors in Japanese men," *Diabetes Care*, vol. 30, no. 9, pp. 2392–2394, 2007.

[4] T. Yoshizumi, T. Nakamura, M. Yamane, a. H. Islam, M. Menju, K. Yamasaki, T. Arai, K. Kotani, T. Funahashi, S. Yamashita, and Y. Matsuzawa, "Abdominal fat: standardized technique for measurement at CT." *Radiology*, vol. 211, no. 1, pp. 283–286, 1999.

[5] Y. Tsushima, A. Taketomi-Takahashi, H. Takei, H. Otake, and K. Endo, "Radiation exposure from CT examinations in Japan." *BMC Med Imaging*, vol. 10, p. 24, 2010.

[6] R. F. Redberg, "Cancer risks and radiation exposure from computed tomographic scans: how can we be sure that the benefits outweigh the risks?" *Arch Intern Med*, vol. 169, no. 22, pp. 2049–2050, 2009.

[7] K. Boone, D. Barber, and B. Brown, "Imaging with electricity: report of the European Concerted Action on Impedance Tomography," *J Med Eng Technol*, vol. 21, no. 6, pp. 201–232, 1997.

[8] D. T. Nguyen, C. Jin, A. Thiagalingam, and a. L. McEwan, "A review on electrical impedance tomography for pulmonary perfusion imaging." *Physiol Meas*, vol. 33, no. 5, pp. 695–706, 2012.

[9] T. Yamaguchi, K. Maki, and M. Katashima, "Practical human abdominal fat imaging utilizing electrical impedance tomography." *Physiol Meas*, vol. 31, no. 7, pp. 963–978, 2010.

[10] Y. Matsushita, T. Nakagawa, S. Yamamoto, Y. Takahashi, T. Yokoyama, M. Noda, and T. Mizoue, "Associations of visceral and subcutaneous fat areas with the prevalence of metabolic risk factor clustering in 6,292 Japanese individuals: the Hitachi Health Study." *Diabetes care*, vol. 33, no. 9, pp. 2117–2119, 2010.

[11] D. B. Geselowitz, "An application of electrocardiographic lead theory to impedance plethysmography," *IEEE Trans Biomed Eng*, vol. 18, no. 1, pp. 38–41, 1971.

[12] T. F. Yamaguchi, M. Katashima, L. Wang, and S. Kuriki, "Improvement of the image-reconstruction of human abdominal conductivity by impedance tomography considering the bioelectrical anisotropy," *Adv Biomed Eng*, vol. 1, pp. 98–106, 2012.

[13] R. Ihaka and R. Gentleman, "R: {A} Language for Data Analysis and Graphics," *J Comput Graph Stat*, vol. 5, no. 3, pp. 299–314, 1996.

[14] A. Azzalini, "The Skew-normal Distribution and Related Multivariate Families," *Scand J Statist*, vol. 32, no. 2, pp. 159–188, 2005.

[15] H. C. Burger and van Dongen, "Specific electric resistance of body tissues," *Phys Med Biol*, vol. 5, pp. 431–447, 1961.

[16] T. J. Faes, H. A. van der Meij, J. C. de Munck, and R. M. Heethaar, "The electric resistivity of human tissues (100 Hz-10 MHz): a meta-analysis of review studies," *Physiol Meas*, vol. 20, no. 4, pp. 1–10, 1999.